

Unified Open-Vocabulary Dense Visual Prediction

Hengcan Shi, Munawar Hayat, and Jianfei Cai,

Abstract—In recent years, open-vocabulary (OV) dense visual prediction (such as OV object detection, semantic, instance and panoptic segmentations) has attracted increasing research attention. However, most of existing approaches are task-specific and individually tackle each task. In this paper, we propose a Unified Open-Vocabulary Network (UOVN) to jointly address four common dense prediction tasks. Compared with separate models, a unified network is more desirable for diverse industrial applications. Moreover, OV dense prediction training data is relatively less. Separate networks can only leverage task-relevant training data, while a unified approach can integrate diverse training data to boost individual tasks. We address two major challenges in unified OV prediction. Firstly, unlike unified methods for fixed-set predictions, OV networks are usually trained with multi-modal data. Therefore, we propose a multi-modal, multi-scale and multi-task (MMM) decoding mechanism to better leverage multi-modal data. Secondly, because UOVN uses data from different tasks for training, there are significant domain and task gaps. We present a UOVN training mechanism to reduce such gaps. Experiments on four datasets demonstrate the effectiveness of our UOVN.

Index Terms—open-vocabulary, object detection, image segmentation.

I. INTRODUCTION

Dense visual prediction tasks, including object detection, semantic, instance and panoptic segmentations, are important and fundamental computer vision problems. They serve as crucial steps for many real-world applications, such as scene understanding [1], [2], image generation [3], [4] and multi-modal systems [5]–[8]. Traditional dense prediction methods [9], [10] are usually designed to recognize a fixed set of object categories. As a result, they have to be continually retrained to fit different real-world applications, because different applications normally involve varying category sets. Hence, open-vocabulary (OV) dense prediction [11], [12] has attracted increasing attention in recent years, where the model is trained to recognize an open set of object categories and thus can be directly used for diverse applications.

The existing OV approaches can be mainly divided into three categories. The first is pre-training-based methods [13]–[16], which learn dense predictions from traditional fixed-set dense data and leverage feature spaces from pre-trained vision-language models to recognize open-set objects. While these methods can generalize to open-vocabulary tasks, pre-trained models reduce the flexibility of these methods. They have to encode their features into the pre-trained feature space and cannot flexibly adjust them. The second category is pseudo-label-based methods [17]–[19], which first generate open-set dense pseudo labels from vision-language data, and then use

these pseudo labels to train OV networks. Nevertheless, these methods suffer from the problem of inevitable noises in pseudo labels. The third type [20], [21] reformulates object detection and segmentation as referring grounding problems, and thus can leverage referring grounding training data to simultaneously enable the dense prediction and OV abilities. Such approaches avoid the noise in pseudo-label-based methods and are more flexible than pre-training-based methods. However, all these three types of methods only focus on one or several dense prediction tasks.

The limitation of the existing OV methods motivates us to look for a unified model for all detection and segmentation tasks, which is more desirable for real-world applications. In addition, compared with traditional fixed-set dense prediction, the training data for OV dense prediction is relatively less. A unified network enables the integration of the training data across different tasks, and thus can enhance the individual performance of each task. Note that there are several recent networks [22]–[26] successfully unifying traditional fixed-set detection and segmentation, demonstrating the feasibility of the unification. However, they cannot be directly used for OV scenarios, due to the lack of OV recognition and training mechanisms.

In particular, in this paper, we propose a Unified Open-Vocabulary Network (UOVN), including an MMM (multi-modal, multi-scale and multi-task) decoding mechanism to jointly detect and segment OV objects, and a UOVN training mechanism to reduce the domain and task gaps in OV training. We adopt the referring-grounding-based mechanism to recognize OV categories. During training, our inputs are an image and language queries which describe some objects in the image. Our MMM decoding generates bounding boxes and/or diverse segmentation masks. During inference, language queries can be replaced with object categories on the target dataset. Inspired by traditional unification works [22], [25], our MMM decoding formulates all detection, semantic, instance and panoptic segmentations into a mask classification problem. We first extract instance-level and pixel-level embeddings, and then generate detection and segmentation results from them. More importantly, we present a multi-modal multi-scale deformable attention (MMDA) module to better extract embeddings based on vision-language information.

We use referring detection and segmentation training data for our model. There are significant domain and task gaps. Therefore, we propose a UOVN training mechanism to address such gaps. We expect to learn domain-invariant embeddings for training samples from different datasets. Traditional domain adaptation methods [27], [28] usually input training samples in the same category into a batch, and make their features similar. However, in our training data, we only have language queries available instead of categories. We observe

H. Shi, M. Hayat, and J. Cai are with the Department of Data Science & AI, Monash University, Melbourne 3800, Australia (e-mail: Hengcan.Shi@monash.edu; Munawar.Hayat@monash.edu; Jianfei.Cai@monash.edu).

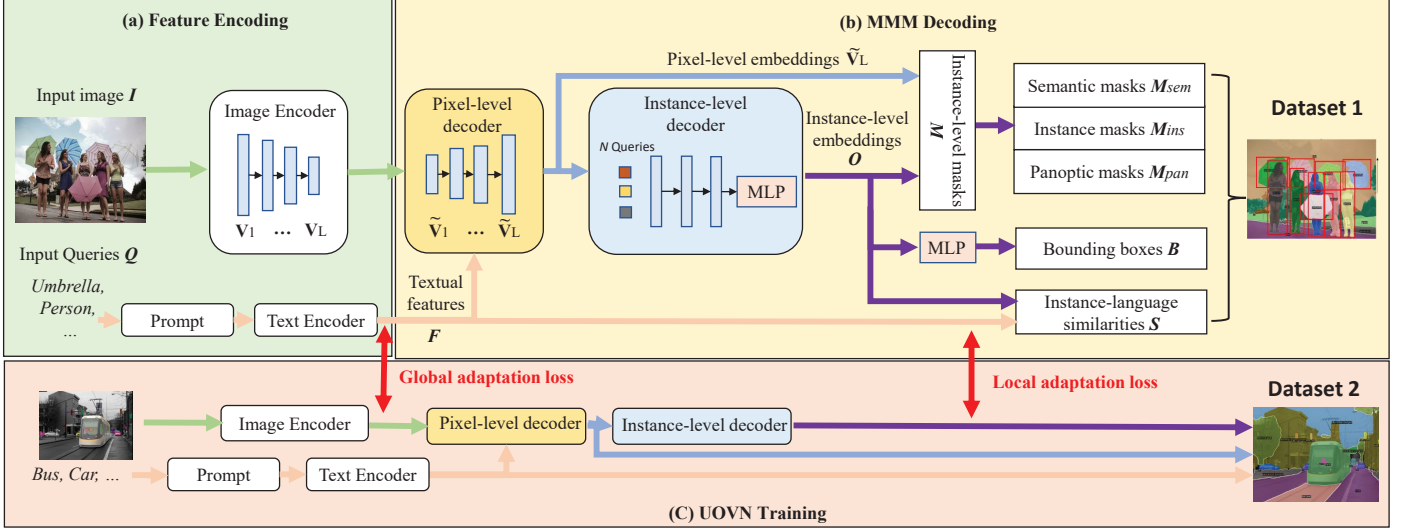


Fig. 1. Illustration of our UOVN. Our model consists of three parts. (a) Feature encoding, including an image encoder and a text encoder, extracts image and text features. (b) MMM (multi-modal, multi-scale and multi-task) decoding, containing a pixel-level decoder and an instance-level decoder, generates OV detection and segmentation results. We also propose a multi-modal multi-scale deformable attention (MMDA) module in this part, to better model multi-modal information. (c) UOVN training leverages different datasets to train our network. We introduce global and local adaptation losses to extract domain-invariant visual embeddings.

that if two images have similar queries, they likely contain similar content. Based on such observation, we introduce global and local adaptation losses, which essentially leverage the textual similarity to guide the visual learning to generate domain-invariant embeddings.

In summary, our major contributions are as follows.

- 1) We propose a novel unified network for OV object detection and diverse segmentation tasks.
- 2) We introduce an MMM decoding and a UOVN training mechanism. The MMM decoding including an MMDA module leverages multi-modal information and the mask classification architecture to enable OV detection, semantic, instance and panoptic segmentations. The UOVN training mechanism allows global and local adaptations among various datasets.
- 3) Extensive experiments on COCO, LVIS, ADE20k and Pascal Context show that our network achieves significant improvements.

II. RELATED WORK

A. Unified Networks for Detection and Segmentation

Object detection, semantic, instance and panoptic segmentations are typical dense visual prediction tasks and widely used in practice. Detection methods [29]–[31] localize and classify objects in an image. Semantic segmentation methods [32]–[35] determine the mask for each object category, which is achieved usually by classifying each pixel in the image. Unlike semantic segmentation, instance segmentation approaches [9], [10] predict masks for different object instances. Panoptic segmentation methods generate instance-level masks for foreground ‘thing’ objects and category-level masks for background ‘stuff’ objects. Earlier panoptic segmentation approaches [36], [37] use two networks to separately

predict instance-level and category-level masks. UPSNet [38] designs a shared encoder with different segmentation heads to solve the panoptic segmentation problem. Since both detection and instance segmentation are instance-level prediction problems, many works [10], [39] use a single instance-level network to unify them. To unify segmentation tasks, recent works [22]–[26] reformulate different segmentation tasks as a mask prediction problem. Several methods [40]–[42] consider detection and segmentation as a (text) sequence prediction problem to flexibly unify them with other tasks, but they do not outperform mask-prediction-based approaches. These fixed-category unified approaches are foundations of our work. However, they cannot be directly used in OV tasks, due to the lack of OV recognition and training mechanisms.

B. Open-Vocabulary Detection and Segmentation

The existing OV detection and segmentation works can be generally categorized into three types. The first is pre-training-based approaches. They normally train their models with fixed-set detection/segmentation data to segment/localize objects, and simultaneously distill knowledge from pre-trained vision-language models to recognize OV categories. For example, [13], [43], [44] use image-caption data to pre-train models for OV detection [13] and semantic segmentation [43], [44]. Many methods [14], [15] employ off-the-shelf vision-language pre-trained models, such as CLIP [45]. ViLD [14] and OV-DETR [46] distill knowledge from CLIP to Mask RCNN [10] and DETR [47], respectively, to predict open-vocabulary detection results. HierKD [15] further embeds multi-level object features and global image features into the CLIP feature space. F-VLM [48] add simple classification heads and localization heads to CLIP, and fine-tune their models on detection data. DetPro [11] incorporates prompt learning to boost the performance,

and Promptdet [49] further enhances the prompt learning to region level. Promptdet [49] is also trained with web images to obtain more knowledge. MaskCLIP-panoptic [50] designs mask class tokens and relative mask attention to better distill CLIP knowledge for OV panoptic segmentation. ODISE [16] employs pre-trained diffusion models to learn open-vocabulary knowledge. These methods successfully leverage vision-language pre-training to improve their OV recognition ability. Nevertheless, their flexibility is limited by pre-trained models in the sense that they have to encode their features into the pre-trained feature space and cannot flexibly adjust them.

The second type is pseudo-label-based methods that generate pseudo detection/segmentation labels from image-level OV data, to address the issue of lacking dense OV annotations. In particular, Detic [17] generates pseudo bounding boxes from large image classification datasets. RegionCLIP [51] and VL-PLM [52] extract pseudo boxes from CLIP by using class activation maps (CAMs) or pre-trained RPN [29]. VLDet [53] predicts nouns from image captions and aligns each noun to object proposals generated by pre-trained object detectors. MaskCLIP+ [54] uses CLIP visual encoder to extract pseudo masks for OV semantic segmentation. XPM [19] generates pseudo masks from image captions for instance segmentation. Instead of directly using pseudo labels, OpenSeg [55] and Rasheed *et al.* [56] first output dense predictions and then restore image-level results from these predictions to train their models. Nevertheless, pseudo-labels introduce inevitable noise during learning.

The third category of approaches, referring-grounding-based works, point out the high similarity between OV dense prediction and grounding, and use grounding frameworks to tackle OV dense prediction. Since grounding data includes detection/segmentation annotations for diverse objects, FindIt [20] combines grounding and object detection data to train a model, which shows OV detection ability. X-DETR [57] reformulates object detection and grounding as an instance-text alignment problem, and designs a unified alignment network for both tasks. GLIP [21] enhances the vision-language interaction in the alignment framework, and also collects millions of data for training. GLIPv2 [58] extends GLIP for more tasks, such as instance segmentation and image captioning. X-Decoder [59] integrates grounding, image caption and image segmentation data for OV segmentation. However, all these three types of works cannot simultaneously deal with detection, semantic, instance and panoptic segmentation tasks. Unlike them, we propose a unified network incorporating the developed MMM decoding and UOVN training mechanisms for all these tasks.

III. PROPOSED METHOD

A. Problem Definition and Method Overview

We formulate OV detection/segmentation as a proposal/mask-language alignment problem. Specifically, our inputs are an image $\mathbf{I} \in \mathbb{R}^{H \times W \times D_I}$ and language queries $\mathbf{Q} \in \mathbb{R}^{C \times P \times D_Q}$, where H and W are the height and width of the image, D_I and D_Q are respectively the channel dimensions of the image and text queries, and C is the number of language queries for the image. During training

with referring grounding/segmentation data, C is the number of referring descriptions for an image, where each description can be a word, a phrase or a sentence, describing an object in the image. During inference, C is the number of object categories on the target dataset. P represents the number of words in each language query.

Our method contains three modules, as illustrated in Fig. 1. (a) *Feature encoding*: an image encoder and a text encoder firstly extract image and text features. (b) *MMM (multi-modal, multi-scale and multi-task) decoding*: in this module, we first output N instance-level bounding boxes, masks and corresponding visual embeddings. Then, C textual embeddings are generated for language queries. After that, we construct a vision-language similarity matrix $\mathbf{S} \in \mathbb{R}^{N \times C}$, which measures the similarity between each object visual embedding and each query textual embedding. The category for each object can be determined by this matrix. Finally, diverse dense predictions are output based on the N instance-level boxes, masks and classification results. (c) *UOVN training*: since various datasets are used during training, we propose global and local adaptation losses to reduce the domain and task gaps among these datasets. Next, we introduce each module in detail.

B. Feature Encoding

Language query encoder. For input queries $\mathbf{Q} \in \mathbb{R}^{C \times P \times D_Q}$, we leverage a textual encoder (e.g., BERT [60] or RoBERTa [61]) to generate a textual feature map $\mathbf{F} \in \mathbb{R}^{C \times D_F}$. In this feature map, each vector $\mathbf{f}_c \in \mathbb{R}^{D_F}$ ($c = 1, \dots, C$) encodes a language query, and D_F is its dimension. Prompt technologies, such as the hand-crafted prompt ‘a photo of a [Query]’ [45] or learnable prompt [62], can be used to further enhance textual features.

Image encoder. We use an image encoder (ResNet [63] or Swin Transformer [64]) to extract multi-scale feature maps $\{\mathbf{V}_l \in \mathbb{R}^{H_l \times W_l \times D_l}\}_{l=1}^L$ for the input image, where L is the number of scales. Feature maps of different scales are extracted from different stages of the image encoder. H_l , W_l and D_l are the height, width and channel number for the l -th feature map, respectively.

C. Multi-modal Multi-scale Multi-task Decoding

We expect to design a unified and clean decoding mechanism for OV dense prediction tasks. Inspired by the recent unified framework Mask2Former [25], we follow its two-decoder architecture: a pixel-level decoder and an instance-level decoder to generate pixel- and instance-level embeddings, respectively. The results of different tasks can be formulated as different combinations of these embeddings.

MMDA module. In Mask2Former [25], the pixel-level decoder is a vision transformer to integrate multi-scale image features and generate pixel-level embeddings. However, in OV scenarios, language cues are also important. Thus, we propose a multi-modal multi-scale deformable attention (MMDA) module, as shown in Fig. 2, to generate multi-scale pixel-level embeddings based on both vision and language information. In particular, considering there may be multiple language query features, (e.g., 80 queries on the COCO dataset during

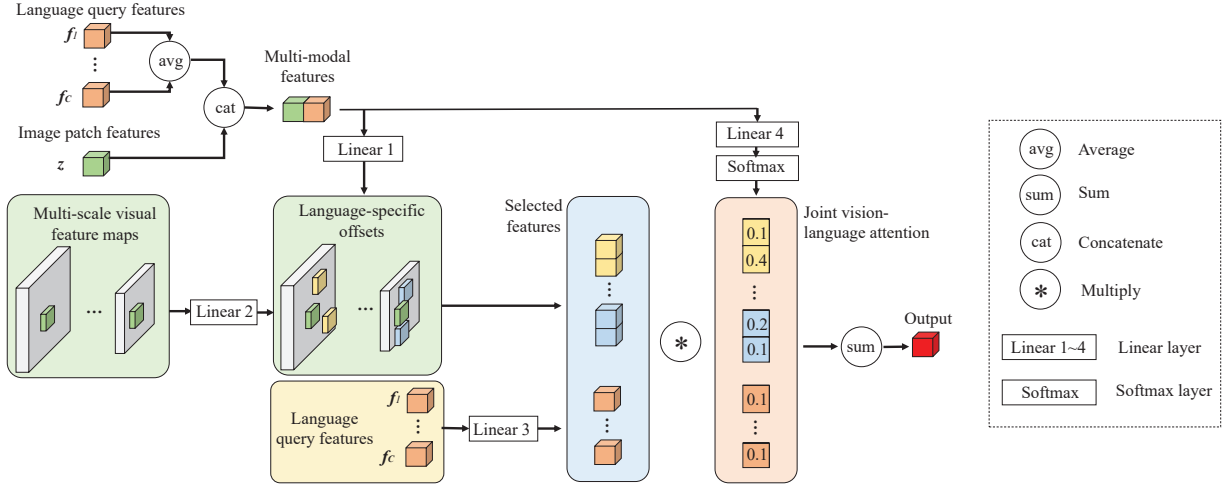


Fig. 2. Illustration of our multi-modal multi-scale deformable attention (MMDA) module, with one attention head for simplicity. We integrate both vision and language cues to predict offsets in deformable attention [65], and thus our MMDA can model language-specific visual relationships. Meanwhile, we learn joint vision-language attentions to fuse multi-modal features for better decoding.

inference), we first aggregate all language query features $\{f_c\}_{c=1}^C$ into a single feature vector by average pooling. Then, the aggregated query feature is concatenated with each image patch feature. The concatenated multi-modal feature is used to predict offsets and compute attention maps in multi-scale deformable attention [65].

Unlike original self-attention, which models relationships among all image patches, deformable attention [65] only models the relationships among K selected patches for every image patch \mathbf{z} to reduce computational costs. It uses a linear layer (‘Linear 1’ in Fig. 2) to predict K offsets to select patches. In our MMDA, the K offsets are predicted by both vision and language cues to model *language-specific visual relationships*. For multi-scale image features, we select K patches on each scale. Finally, for every image patch \mathbf{z} , a set of $K \times L$ selected patch feature vectors is constructed. To further model vision-language information, we also add language query features to this set. Note that all features in this set are transformed by linear layers (‘Linear 2&3’ in Fig. 2) as ‘values’ in attention model.

A linear layer (‘Linear 4’ in Fig. 2) and a softmax are used to calculate attention maps. These attention maps measure the importance of every feature vector in the selected feature set, where we also leverage both vision and language cues to learn *joint vision-language attention*. The output of one attention head is a weighted sum of features in the set, where the weights are from the attention map. In each Transformer layer, we use eight attention heads and integrate their outputs into one feature vector.

Detection and segmentation output generation. The outputs of the pixel-level decoder are transformed feature maps $\{\tilde{\mathbf{V}}_l \in \mathbb{R}^{H_l \times W_l \times D_F}\}_{l=1}^L$, where D_F is their dimension, same as the dimension of textual features. Each of these feature maps incorporates multi-scale vision and language information. Similar to Mask2Former [25], we use a Transformer decoder with masked attention and a two-layer MLP (Multi-layer perceptron) as our instance-level decoder. It takes multi-

scale features maps $\{\tilde{\mathbf{V}}_l\}_{l=1}^{L-1}$ generated from the pixel-level decoder as key and value, and includes N learnable Transformer queries. The outputs are instance-level embeddings $\mathbf{O} \in \mathbb{R}^{N \times D_F}$, where D_F is the dimension. Each feature vector $\mathbf{o}_n \in \mathbb{R}^{D_F}$ ($n = 1, \dots, N$) in \mathbf{O} embeds an object instance.

We then generate dense predictions from the pixel- and instance-level embeddings $\tilde{\mathbf{V}}_L$ and \mathbf{O} . Specifically, segmentation masks can be predicted as

$$\mathbf{M} = \text{Binary}(\text{Sigmoid}(\mathbf{O}\tilde{\mathbf{V}}_L^T)) \quad (1)$$

where T means a tensor transposition, and $\text{Sigmoid}(\cdot)$ and $\text{Binary}(\cdot)$ are sigmoid and binary thresholding functions, respectively. In the binary thresholding function, if a value is higher than 0.5, we set it to 1; otherwise 0. $\mathbf{M} \in \mathbb{R}^{N \times H_L \times W_L}$ are segmentation masks for N object instances and each mask is a binary one of $H_L \times W_L$. These segmentation masks can be directly used as *instance segmentation results* \mathbf{M}_{ins} .

The similarity matrix $\mathbf{S} \in \mathbb{R}^{N \times C}$ between visual instances and language queries can be calculated as

$$\mathbf{S} = \mathbf{O}\mathbf{F}^T. \quad (2)$$

During inference, language queries are object categories of the target dataset. We can also add a ‘no object’ class similar to fixed-set works [24], [47]. For each object instance, we find the class with the highest similarity as its classification result. However, different from fixed-set datasets, in referring grounding/segmentation datasets, an object instance may correspond to multiple language queries, and a language query may describe multiple object instances. Therefore, during training, we calculate binary cross-entropy loss for every element in \mathbf{S} .

Semantic segmentation masks $\mathbf{M}_{sem} \in \mathbb{R}^{C \times H_L \times W_L}$ can be treated as a combination of instance-level segmentation masks \mathbf{M} . Through Eq. (1)&(2), we obtain instance-level masks and their classes. For every class, we fuse instance-level masks of this class as the semantic segmentation results. *Panoptic segmentation* expects to generate instance segmentation results for pre-defined classes, while semantic segmentation results

for other classes. Therefore, we can combine instance and semantic segmentation results based on their classes as panoptic segmentation results \mathbf{M}_{pan} .

A simple way to predict *object detection* results is via a post-processing step to directly generate bounding boxes from instance segmentation masks. However, to better leverage bounding-box-only annotations during training, we add an additional two-layer MLP to generate bounding boxes $\mathbf{B} \in \mathbb{R}^{N \times 4}$ based on instance-level embeddings \mathbf{O} .

D. UOVN Training

We train our network jointly with segmentation, detection, classification and adaptation losses:

$$L = \lambda_1 L_{seg} + \lambda_2 L_{det} + \lambda_3 L_{cls} + \lambda_4 L_{adp}, \quad (3)$$

where L_{seg} is for mask predictions, L_{det} is the detection loss for the bounding box regression, L_{cls} is for OV classification, and L_{adp} is for the adaptation in cross-dataset training. $\lambda_1, \lambda_2, \lambda_3$ and λ_4 are hyperparameters to weight different losses. Note that our losses can be flexibly adjusted according to the training data, e.g., the segmentation loss can be removed when only box annotations are given.

Specifically, we use the common detection loss [47] as our L_{det} , which minimizes the *smooth l_1 distance* and *GIoU* between ground truths and bounding box predictions \mathbf{B} . The segmentation loss in [24], [25] is employed as our L_{seg} to optimize the *binary cross-entropy* and *Dice* between mask predictions \mathbf{M} and ground truths. Bipartite Hungarian matching is used to align predicted boxes/masks with ground truths. The OV classification loss L_{cls} is a binary cross-entropy between the similarity matrix and the ground truth matrix:

$$L_{cls} = L_{BCE}(\mathbf{S}_{gt}, \text{Sigmoid}(\mathbf{S})) \quad (4)$$

where the ground truth (GT) matrix $\mathbf{S}_{gt} \in \mathbb{R}^{N \times C}$ is generated from mask/box labels and their corresponding language queries. Specifically, we set GT similarity $s_{n,c}$ to 1, when the IoU between the n -th predicted mask/box and the GT mask/box of the c -th query is larger than 0.5; otherwise, we set it to 0.

Adaption loss. The adaption loss L_{adp} is proposed to learn domain-invariant embeddings to reduce cross-dataset gaps, which consists of two parts: $L_{adp} = L_{adp-g} + L_{adp-l}$. L_{adp-g} is a global adaption loss to capture image-level domain-invariant embeddings, while L_{adp-l} represents a local adaption loss for learning instance-level domain-invariant embedding. Fixed-set domain adaptation methods [27], [28] often extract domain-invariant features by inputting images from different datasets but in the same category into a batch, and making their features similar. However, our training data only includes language queries rather than image categories. We notice that if two images have similar queries, they likely share similar content, and vice versa. Based on this observation, we propose to use the textual similarity to guide the visual similarity learning for domain adaptation.

Concretely, we first input two image-query pairs from different datasets into a batch. Then, we compute the visual similarity a_v between the images and the textual similarity

a_l between language queries. Considering an image may have multiple language queries, we average query features $\{\mathbf{f}_c\}_{c=1}^C$ into a single vector $\mathbf{f} \in \mathbb{R}^{D_F}$. The visual feature map $\mathbf{V}_L \in \mathbb{R}^{H_L \times W_L \times D_L}$ in the last stage of the image encoder is also averaged into a vector $\mathbf{v} \in \mathbb{R}^{D_L}$. After that, we compute a_v as the cosine similarity between the averaged visual features of the two images, and a_l as the cosine similarity between the two averaged query features. The global adaption loss L_{adp-g} then matches the visual and textual similarities:

$$L_{adp-g} = L_{dis}(a_v, a_l). \quad (5)$$

Since a_v and a_l are two numbers, we use the ℓ_1 -norm distance as our loss function L_{dis} . We encourage the visual embeddings of two images from different datasets to have a similar distance as that of their queries embeddings.

Similarly, we can apply the same adaptation idea at the instance level. For two objects from different datasets, we make their visual similarity to be close to the textual similarity between their corresponding queries. In particular, we first generate the language similarity matrix $\mathbf{A}_L \in \mathbb{R}^{C_1 \times C_2}$ between the two training samples from different datasets: $\mathbf{A}_L = \mathbf{F}^1(\mathbf{F}^2)^T$, where $\mathbf{F}^1 \in \mathbb{R}^{C_1 \times D_F}$ and $\mathbf{F}^2 \in \mathbb{R}^{C_2 \times D_F}$ are the language query feature maps in the two training samples, respectively, and C_1 and C_2 are their numbers of queries. Then, based on the cross-modal similarity matrix \mathbf{S} in Eq.2, we can get the instance embedding corresponding to each language query. If a query corresponds to multiple instances, we average their embeddings. In this way, we can obtain two instance embedding matrices $\tilde{\mathbf{O}}^1 \in \mathbb{R}^{C_1 \times D_F}$ and $\tilde{\mathbf{O}}^2 \in \mathbb{R}^{C_2 \times D_F}$ for the two training samples, respectively, and compute the visual similarity matrix $\mathbf{A}_V = \tilde{\mathbf{O}}^1(\tilde{\mathbf{O}}^2)^T$, where $\mathbf{A}_V \in \mathbb{R}^{C_1 \times C_2}$. The local adaptation loss L_{adp-l} is then given by

$$L_{adp-l} = L_{KL}(\mathbf{A}_L, \mathbf{A}_V) \quad (6)$$

where we use a Kullback-Leibler divergence loss L_{KL} to constrain the similarity between the two matrices \mathbf{A}_L and \mathbf{A}_V .

IV. EXPERIMENTS

A. Experiment Settings

Following previous OV methods [11], [14], [50], we evaluate UOVN at two scenarios: *cross-dataset* and *zero-shot*. Note that there is no single training setting used across existing OV methods, since OV methods focus on using unrestricted training data to recognize unseen objects. Most of the existing approaches collect different training data and/or pre-training models. For a fair comparison, we reproduce key baselines on our training data.

Cross-dataset scenario. This scenario uses different training and testing datasets to gauge the OV ability. To train our model, we combine widely used referring grounding/segmentation datasets: RefCOCO [69], ReferItGame [70], Visual Genome [71] and PhraseCut [72]. As prior works [11], [14], [46] usually use LVIS base (886 common and frequent classes) [73] for training, we also include these data in our training set. We have 300K training samples in total. Our goal is to verify the effectiveness of our unified network rather than

TABLE I

CROSS-DATASET RESULTS ON COCO VALIDATION. ‘DET’, ‘INS’ AND ‘PAN’ ARE OBJECT DETECTION, INSTANCE AND PANOPTIC SEGMENTATIONS, RESPECTIVELY. ‘×’ MEANS THE METHOD CANNOT DEAL WITH THIS TASK. ‘SD’ IS STABLE DIFFUSION MODEL. ‘MODEL A’ IS A MODIFIED MASK2FORMER [25], WHERE WE REPLACE THE CLASSIFICATION PART WITH A VISION-LANGUAGE SIMILARITY MATRIX FOR OV RECOGNITION. OUR UOVN IS ABLE TO DEAL WITH ALL DETECTION AND SEGMENTATION TASKS, AND OUTPERFORMS MOST OF THE PREVIOUS APPROACHES. GLIP [21] USE LARGER BACKBONES AND MUCH MORE TRAINING/PRE-TRAINING DATA. X-DECODER [59] AND ODISE [16] ARE FULLY-SUPERVISED ON COCO.

Method	Backbone	Supervision		Det	Ins	Pan
		VL Pre-training	Training	mAP	mAP	PQ
ViLD [14]	Res-50	400M (CLIP)	100K (LVIS base)	36.6	×	×
DetPro [11]	Res-50	400M (CLIP)	100K (LVIS base)	34.9	×	×
OV-DETR [46]	Res-50	400M (CLIP)	100K (LVIS base)	38.1	×	×
X-DETR [57]	Res-101	-	14M (grounding, detection, caption)	26.5	×	×
GLIP [21]	Swin-L	-	27M (grounding, detection, caption)	49.8	×	×
X-Decoder [59] (fully-supervised)	Focal-T	-	4M (caption, grounding, COCO Pan)	×	46.7	56.9
ODISE [16] (fully-supervised)	SD	400M (SD) + 400M (CLIP)	240K (COCO Cap, COCO Pan)	×	×	55.4
GLIP [21] (re-train)	Res-50	-	300K (grounding, LVIS base)	35.4	×	×
Model A (modified Mask2Former [25])	Res-50	-	300K (grounding, LVIS base)	×	20.8	24.4
UOVN (Ours)	Res-50	-	300K (grounding, LVIS base)	41.3	30.5	32.7

train a large pre-training model. Thus, we do not use millions of training data like pre-training works [21]. Following prior works [14], [50], we take COCO [74], ADE20K [75] and Pascal Context [76] as testing datasets. There are overlapped images between COCO and LVIS/grounding datasets. Although most of the prior works use these overlapped images during training, we remove them from our training data to better verify the OV ability.

Zero-shot scenario. In this scenario, the training and testing are on the same dataset, but with disjoint classes. We report zero-shot results on COCO [74] and LVIS [73]. For the COCO [74] dataset, we use the grounding data and COCO base (48 base classes) for training, while testing our model on 17 COCO novel classes. For LVIS [73], our training data the combination of grounding data and LVIS base (886 common and frequent classes). The testing set is 337 LVIS rare classes. We not only exclude overlapped images from our training data, but also remove language queries which contain target classes in testing sets.

Metrics. We use $mIoU$ for semantic segmentation, mAP and AP^{50} for detection and instance segmentation, as well as PQ for panoptic segmentation [36].

B. Dataset Details

Grounding datasets. We use RefCOCO [69], ReferItGame [70], Visual Genome [71] and PhraseCut [72] grounding data to enable the OV recognition ability. Both RefCOCO [69] and ReferItGame [70] contain 20K images. Visual Genome [71] and PhraseCut [72] have 108K and 77K images, respectively. Visual Genome [71] provides bounding box annotations with phrase and word descriptions. RefCOCO [69] contains both bounding box and segmentation annotations, but only ‘things’ objects are labeled. ReferItGame [70] and PhraseCut [72] provide bounding box and segmentation annotations for both ‘things’ and ‘stuff’ objects.

COCO. COCO 2017 [74] contains 120K training and 5K validation images for the detection, instance and panoptic segmentation tasks. There are 80 object classes for detection and instance segmentation, as well as 133 object classes in

panoptic segmentation. 48 base classes and 17 novel classes are selected as the same in [77] for zero-shot evaluation.

ADE20K. We use the ADE20K [75] dataset during testing. 2K validation images in this dataset are annotated for semantic and panoptic segmentations, and objects are divided into 847 or 150 classes.

Pascal Context. The Pascal Context [76] dataset is a semantic segmentation benchmark. There are 5.1K validation images and two kinds of class definitions: 459 and 59 classes.

LVIS. LVIS [73] includes object detection and instance segmentation annotations for 100K training and 20K validation images. Object categories in LVIS [73] are split into three sets: 405 frequent, 461 common and 337 rare classes. We use 886 frequent and common classes as base classes for training, while taking 337 rare classes for zero-shot testing.

C. Implementation Details

We choose RoBERTa [61] as our text encoder and add a linear layer to convert the textual feature dimension D_F to 256. We fix RoBERTa during training and only update the parameters of the linear layer. We do not use any prompt during training, only the prompt ‘A photo of a [query]’ is used during inference. Res-50 [63] pre-trained on ImageNet is used as our image encoder, because most of the previous methods [14], [19], [50] employ it. Feature maps on four scales (i.e., $L = 4$) are extracted. In our MMDA module, we set the number K of patches to 4. In the instance-level decoder, 100 instance embeddings are generated, i.e., $N = 100$. For the adaptation training, we randomly input two images from different datasets into a batch. λ_1 , λ_2 , λ_3 and λ_4 are simply set to 2.0, 2.0, 1.0 and 1.0, respectively, and fixed for all datasets. Other network and training settings are the same as Mask2former [25]. Similar to [21], the maximum number of language queries is set to 256. If an image corresponds to over 256 language queries, we divide them into multiple sets and separately generate results for each set. All experiments are conducted on the Pytorch platform [78] with 8 V100 GPUs and 2 images per GPU.

TABLE II

CROSS-DATASET RESULTS ON ADE20K AND PASCAL CONTEXT VALIDATION. ‘A-847’ AND ‘A-150’ MEAN 847 AND 150 CLASSES ON ADE20K, RESPECTIVELY, WHILE ‘P-459’ AND ‘P-59’ MEAN 459 AND 59 CLASSES FOR PASCAL CONTEXT. ‘SEM’ AND ‘PAN’ ARE SEMANTIC AND PANOPTIC SEGMENTATION. ‘X’ MEANS THE METHOD CANNOT DEAL WITH THIS TASK. ‘SD’ IS STABLE DIFFUSION. ONLY ADE20K CONTAINS PANOPTIC SEGMENTATION VALIDATION.

Method	Backbone	Supervision		Sem (<i>mIoU</i>)				Pan (<i>PQ</i>)
		VL Pre-training	Training	A-847	A-150	P-459	P-59	ADE20K
GroupViT [66]	ViT-S	-	27M (caption)	-	-	-	20.4	×
OpenSeg [55]	EfficientNet-B7	1.3B (ALIGN)	240K (COCO Cap, COCO)	6.3	21.1	9.0	42.1	×
Xu <i>et al.</i> [67]	Res-101	400M (CLIP)	120K (COCO-stuff)	7.0	20.5	-	47.7	×
MaskCLIP-panoptic [50]	Res-50	400M (CLIP)	120K (COCO Pan)	8.2	23.7	10.0	45.9	15.1
OVSeg [68]	Swin-B	400M (CLIP)	240K (COCO Cap, COCO-stuff)	9.0	29.6	12.4	55.7	×
X-Decoder [59]	Focal-T	-	4M (caption, grounding, COCO Pan)	9.2	29.6	16.1	64.0	21.8
ODISE [16]	Swin-L	400M (SD) + 400M (CLIP)	240K (COCO Cap, COCO Pan)	11.1	29.9	14.5	57.3	22.6
Model A (modified Mask2Former [25])	Res-50	-	300K (grounding, LVIS base)	7.6	22.0	9.8	42.2	16.8
UOVN (Ours)	Res-50	-	300K (grounding, LVIS base)	13.5	30.7	17.1	54.3	23.9

TABLE III

ZERO-SHOT RESULTS ON COCO. ‘DET’ AND ‘INS’ ARE DETECTION AND INSTANCE SEGMENTATION. WE USE THE GENERALIZED ZERO-SHOT SETTING [77]. ‘X’ MEANS THE METHOD DOES NOT DEAL WITH THE TASK. NOTE THAT SEVERAL METHODS [49], [53], [56] USE NOVEL-CLASS INFORMATION DURING TRAINING, WHICH IS NOT PRACTICAL FOR THE OV TASK.

Method	Backbone	VL Pre-training	Training	Det (AP^{50})			Ins (AP^{50})			
				novel	base	all	novel	base	all	
<i>without novel classes:</i>										
OVR-CNN [13]	Res-50	-	240K (COCO Cap, COCO base)	22.8	46.0	39.9				×
Detic [17]	Res-50	400M (CLIP)	240K (COCO Cap, COCO base)	27.8	47.1	45.0				×
ViLD [14]	Res-50	400M (CLIP)	120K (COCO base)	27.6	59.5	51.3				×
XPM [19]	Res-50	-	5.1M (caption, OI, COCO base)	29.9	46.3	42.0	21.9	41.5	36.3	
OV-DETR [46]	Res-50	400M (CLIP)	120K (COCO base)	29.4	61.0	52.7				×
RegionCLIP [51]	Res-50	400M (CLIP)	3M (CC, COCO base)	31.4	57.1	50.4				×
F-VLM [48]	Res-50	400M (CLIP)	120K (COCO base)	28.0	-	39.6				×
GLIP [21] (re-train)	Res-50	-	320K (grounding, COCO base)	27.4	56.2	48.7				×
Model A (modified Mask2Former [25])	Res-50	-	320K (grounding, COCO base)		×		24.5	51.7	44.6	
UOVN (Ours)	Res-50	-	320K (grounding, COCO base)	32.7	62.6	54.2	31.1	54.8	48.6	
<i>with novel classes:</i>										
PromptDet [49]	Res-50	400M (CLIP)	400M (LAION, COCO)	26.6	-	50.6				×
VLDet [53]	Res-50	400M (CLIP)	240K (COCO Cap, COCO)	32.0	50.6	45.8				×
Rasheed <i>et al.</i> [56]	Res-50	400M (CLIP, MViT)	240K (COCO Cap, COCO)	36.6	54.0	49.4				×

D. Main Results

We first report the cross-dataset results on COCO in Table I. Since prior works [14], [19], [50] usually use Res-50 as their backbones, we also use the Res-50 backbone for a fair comparison. GLIP [21] is the first work that reformulates object detection to referring grounding. However, it is trained with 27 million data as a vision-language pre-training. Rather than designing a pre-training, our work aims to provide an architecture for unified OV dense prediction. Therefore, we reproduce GLIP [21] with our 300K training data. Compared with GLIP [21], our method obtains 5.9% gains on the detection task. Moreover, GLIP [21] is only designed for detection, while our method is generic and can generate various segmentation results. We design another baseline called ‘Model A’ where we add a text encoder to Mask2former [25] and replace the classification part in Mask2former [25] with a vision-language similarity matrix for OV recognition. This model can only deal with segmentation tasks and is trained on segmentation data. Due to referring segmentation data being relatively less, the performance of ‘Model A’ is impacted. Our unified network flexibly combines referring detection and segmentation data for training, and we also propose MMM decoding and UOVN training mechanisms. Therefore, our method achieves significant improvements as well as outperforms most of other state-of-the-art approaches. The original GLIP [21] performs better

because of a larger backbone and millions of training/pre-training data. X-Decoder [59] and ODISE [16] report superior COCO segmentation results, but they are fully-supervised for COCO.

Table II shows the segmentation results on ADE20K and Pascal Context. GLIP [21] cannot generate segmentation results. Our method brings remarkable improvements, compared to baseline ‘Model A’. X-Decoder [59] and ODISE [16] show the best performance in prior works, while our method outperforms them under most metrics, especially for a mass of classes (e.g., 847 and 459 classes). These results demonstrate our OV ability, built upon our proposed MMM decoding to integrate multi-modal OV data and adaptation losses to reduce cross-dataset gaps. Instead of OV recognition, X-Decoder [59] focuses on segmentation, and uses more segmentation labels as well as an elaborate backbone. Therefore, it shows higher IoU when segmenting 59 classes, which are almost covered by their segmentation labels.

Table III and Table IV report the zero-shot results on COCO and LVIS. UOVN achieves significant improvements, compared to other state-of-the-art methods with the same backbone. Note that several works [49], [53], [56] use a different setting that involves novel-class information of the target dataset. Concretely, they generate pseudo training samples based on novel classes of the target dataset, which is not

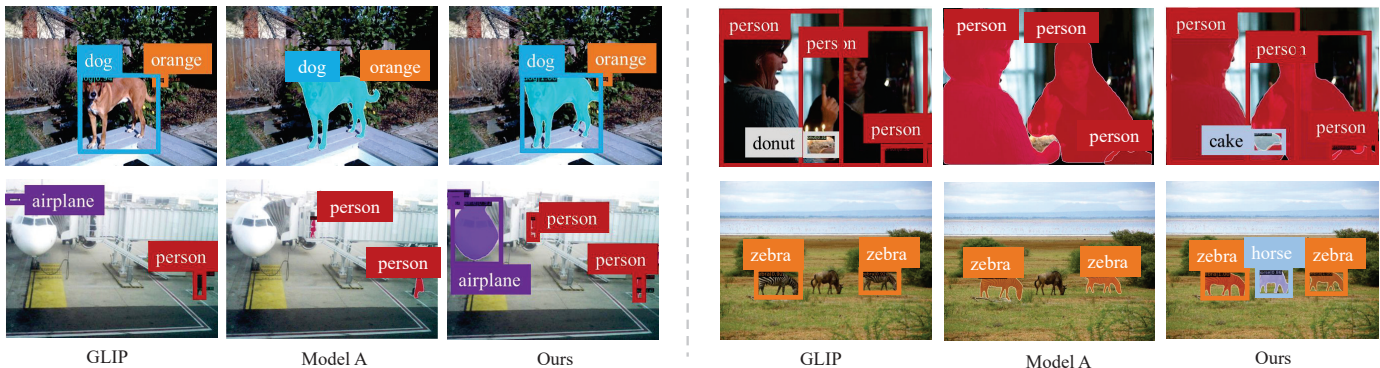


Fig. 3. Qualitative cross-dataset object detection and instance segmentation results on COCO validation. Re-trained GLIP [21] and ‘Model A’ ignore and mis-classify objects, such as the ‘cake’ in the upper right image as well as the ‘horse’ in the bottom right image. Our method can detect, segment and recognize these objects.

TABLE IV

ZERO-SHOT RESULTS ON LVIS. ‘DET’ AND ‘INS’ ARE DETECTION AND INSTANCE SEGMENTATION. ‘X’ MEANS THIS METHOD DOES NOT TACKLE THIS TASK. NOTE THAT SEVERAL METHODS [49], [53], [56] USE NOVEL-CLASS INFORMATION DURING TRAINING, WHICH IS NOT PRACTICAL FOR THE OV TASK.

Method	Backbone	VL Pre-training	Training	Det (mAP)				Ins (mAP)				
				rare	common	frequent	all	rare	common	frequent	all	
<i>without novel classes:</i>												
Detic [17]	Res-50	400M (CLIP)	240K (COCO Cap, COCO base)			×		17.8	26.3	31.6	26.8	
ViLD [14]	Res-50	400M (CLIP)	100K (LVIS base)			×		16.6	24.6	30.3	25.5	
DetPro [11]	Res-50	400M (CLIP)	100K (LVIS base)	20.8	27.8		32.4	19.8	25.6	28.9	25.9	
OV-DETR [46]	Res-50	400M (CLIP)	100K (LVIS base)			×		17.4	25.0	32.5	26.6	
RegionCLIP [51]	Res-50	400M (CLIP)	3M (CC, LVIS base)			×		17.1	27.4	34.0	28.2	
F-VLM [48]	Res-50	400M (CLIP)	100K (LVIS base)			×		18.6	-	-	24.2	
GLIP [21] (re-train)	Res-50	-	300K (grounding, LVIS base)	18.9	27.0		31.2	26.9		×		
Model A (modified Mask2Former [25])	Res-50	-	300K (grounding, LVIS base)			×		15.7	28.1		33.4	
UOVN (Ours)	Res-50	-	300K (grounding, LVIS base)	22.6	31.9		37.1	32.0	22.0	30.7	35.7	30.9
<i>with novel classes:</i>												
PromptDet [49]	Res-50	400M (CLIP)	400M (LAION, LVIS)			×		21.4	23.3	29.3	25.3	
VLDet [53]	Res-50	400M (CLIP)	3M (CC, LVIS)			×		21.7	29.8	34.3	30.1	
Rasheed <i>et al.</i> [56]	Res-50	400M (CLIP, MViT)	1.5M (ImageNet21K, LVIS)			×		21.1	25.0	29.1	25.9	

practical from the OV perspective. Nevertheless, our method also outperforms most of them. All these superior results demonstrate the effectiveness of our unified network, as well as our proposed MMM decoding and adaptation strategies.

E. Discussion

In this section, we conduct a series of discussions to further verify the effectiveness of every module in our UOVN, including (1) the effects of each main component, (2) different settings of the MMDA module and (3) UOVN training, (4) task analysis, (5) the effects of prompt, as well as (6) the analysis of qualitative results.

Main components. We report ablation study results in Table V. Compared with our baseline ‘Model A’, our MMM decoding first incorporates a detection branch (‘Model C’) which allows joint training on both detection and segmentation data. Through the joint training, the instance and panoptic segmentation results are increased by 5.4% and 3.4%. The MMDA module (‘Model D’) in our decoding yields improvements of 2.6%, 2.2% and 3.0% on the detection, instance and panoptic segmentation tasks, respectively. The UOVN training strategy (‘Full Model’) improves the performance by 1.7%, 2.1% and 1.9% for detection, instance and panoptic segmentations. These results demonstrate the effectiveness of our MMM decoding, MMDA module and UOVN training.

MMDA module. We then dissect our MMDA module. The results are shown in Table VI. In ‘Model E’, we only use language query to guide the deformable offset generation. In ‘Model F’, we exclude language features from the selected feature set and only use vision cues to calculate attentions. Compared with the model without MMDA (‘Model C’), both ‘Model E’ and ‘Model F’ increase the performance of all tasks, because our language-specific offsets and joint vision-language attention in MMDA better learn visual embedding from language cues. The entire MMDA module (‘Model D’) further improves the performance.

UOVN training. As our training data comes from diverse domains and tasks, we propose a global adaptation loss L_{adp-g} and a local adaptation loss L_{adp-l} to reduce domain gaps. Table VII shows the effects of L_{adp-g} and L_{adp-l} . Compared with ‘Model D’, our L_{adp-g} and L_{adp-l} improve the detection performance by 0.8% and 1.1%, respectively. These losses also show improvements on other tasks. Meanwhile, the local adaptation loss L_{adp-l} yields more improvements than the global adaptation loss L_{adp-g} , because local object embeddings are more crucial for dense prediction tasks. By combining global and local losses, our final model obtains the best performance.

Task analysis. In table V, ‘Model A’ and ‘Model B’ separately use segmentation and detection data for training. Compared with these task-specific models, the unified network

TABLE V

ABLATION STUDY ON COCO VALIDATION AT THE CROSS-DATASET SCENARIO. ‘DET’, ‘INS’ AND ‘PAN’ MEAN DETECTION, INSTANCE AND PANOPTIC SEGMENTATIONS. ‘X’ INDICATES THAT THE METHOD CANNOT TACKLE THIS TASK. IN ‘MODEL A’, WE USE A VISION-LANGUAGE SIMILARITY MATRIX TO REPLACE CLASSIFICATION LAYERS IN MASK2FORMER [25] FOR OV RECOGNITION.

Method	Segmentation tasks	Detection task	MMDA module	UOVN training	Det mAP	Ins mAP	Pan PQ
Model A (modified Mask2Former [25])	✓				×	20.8	24.4
Model B		✓			33.8	×	×
Model C	✓	✓			37.0	26.2	27.8
Model D	✓	✓	✓		39.6	28.4	30.8
Full Model	✓	✓	✓	✓	41.3	30.5	32.7

TABLE VI

THE EFFECTS OF DIFFERENT SETTINGS IN OUR MMDA MODULE. ALL RESULTS ARE ON COCO VALIDATION AT THE CROSS-DATASET SCENARIO. ‘DET’, ‘INS’ AND ‘PAN’ MEAN DETECTION, INSTANCE AND PANOPTIC SEGMENTATIONS.

Method	Language-specific offsets	Joint vision-language attention	Det mAP	Ins mAP	Pan PQ
Model C			37.0	26.2	27.8
Model E	✓		38.1	26.7	29.2
Model F		✓	38.8	27.6	30.3
Model D	✓	✓	39.6	28.4	30.8

TABLE VII

THE EFFECTS OF DIFFERENT SETTINGS IN OUR UOVN TRAINING. ALL RESULTS ARE ON COCO VALIDATION AT THE CROSS-DATASET SCENARIO. ‘DET’, ‘INS’ AND ‘PAN’ MEAN DETECTION, INSTANCE AND PANOPTIC SEGMENTATIONS.

Method	Global adaptation L_{adp-g}	Local adaptation L_{adp-l}	Det mAP	Ins mAP	Pan PQ
Model D			39.6	28.4	30.8
Model G	✓		40.4	28.9	31.5
Model H		✓	40.7	30.2	32.1
Full Model	✓	✓	41.3	30.5	32.7

‘Model C’ yields significant improvements, especially for segmentation tasks, because referring segmentation training data is relatively less than the data for referring detection.

Prompt. Language prompt is a frequently-used technology to enhance language representations in open-vocabulary methods. As described in Section III-B, we use the CLIP prompt ‘A photo of [query]’ during inference. Table VIII shows the results of our method without this prompt. It is seen that prompt slightly improves our performance for all tasks. We also use this prompt in other ablation models (i.e., ‘Model A-H’ and ‘Full Model’).

Qualitative results. We depict qualitative results in Fig. 3 and Fig. 4. In Fig. 3, both re-trained GLIP [21] and ‘Model A’ ignore the largest ‘airplane’ in the bottom left image and the ‘horse’ in the bottom right image. Moreover, GLIP [21] also mis-classifies ‘cake’ as ‘donut’ in the upper right image, and ‘Model A’ cannot segment this object. Different from them, our method successfully detects, segments and recognizes these objects. A reason is that we combine segmentation and detection to recognize objects, and our MMM decoding, MMDA module as well as UOVN training better integrate multi-task, multi-modal and multi-dataset information. Fig. 4 shows the panoptic segmentation results. GLIP [21] is unable to tackle this task. ‘Model A’ cannot segment the ‘zebra’ as

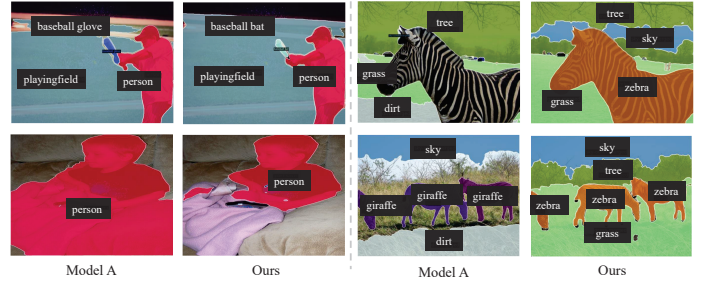


Fig. 4. Qualitative cross-dataset panoptic segmentation results on COCO validation. ‘Model A’ does not well segment some objects, such as the ‘person’ in the bottom left image and the ‘zebra’, ‘tree’ as well as ‘grass’ in the bottom right image. Meanwhile, the ‘baseball bat’ in the upper left image is misclassified as ‘baseball glove’. Our method avoids these errors.

TABLE VIII

THE EFFECTS OF PROMPT ON COCO VALIDATION. ‘DET’, ‘INS’ AND ‘PAN’ MEAN OBJECT DETECTION, INSTANCE AND PANOPTIC SEGMENTATIONS.

Method	Det mAP	Ins mAP	Pan PQ
Ours without prompt	40.5	29.6	31.9
Ours with prompt	41.3	30.5	32.7

well as ‘sky’ in the upper right image, and mis-recognizes ‘grass’ as ‘dirt’. Our method reduces these mistakes, because we incorporate detection data for training, use MMM decoding for better OV object recognition, and propose adaptation to enhance the training.

V. CONCLUSION

In this paper, we have presented UOVN, a unified network for open-vocabulary object detection, semantic, instance and panoptic segmentations. We first introduce a multi-modal, multi-scale and multi-task (MMM) decoding mechanism to recognize open-category objects and generate bounding boxes as well as diverse segmentation masks. In MMM decoding, we propose a multi-modal multi-scale deformable attention (MMDA) module to leverage multi-modal information to enhance extracted embeddings. Secondly, a UOVN training mechanism, including global and local adaptation losses, is presented to reduce domain and task gaps among heterogeneous training data. Extensive experimental results on the COCO, LVIS, ADE20K and Pascal Context datasets demonstrate the effectiveness of our method.

REFERENCES

- [1] L. Ma, H. Xie, C. Liu, and Y. Zhang, "Learning cross-channel representations for semantic segmentation," *IEEE Transactions on Multimedia*, 2022.
- [2] G. Yang, E. Fini, D. Xu, P. Rota, M. Ding, T. Hao, X. Alameda-Pineda, and E. Ricci, "Continual attentive fusion for incremental learning in semantic segmentation," *IEEE Transactions on Multimedia*, 2022.
- [3] L. Zhao, P. Huang, T. Chen, C. Fu, Q. Hu, and Y. Zhang, "Multi-sentence complementarily generation for text-to-image synthesis," *IEEE Transactions on Multimedia*, 2023.
- [4] G. Liu, H. Yue, J. Wu, and J. Yang, "Intra-inter view interaction network for light field image super-resolution," *IEEE Transactions on Multimedia*, 2021.
- [5] Z. Guo, J. Zhao, L. Jiao, X. Liu, and F. Liu, "A universal quaternion hypergraph network for multimodal video question answering," *IEEE Transactions on Multimedia*, 2021.
- [6] H. Shi, H. Li, Q. Wu, and K. N. Ngan, "Query reconstruction network for referring expression image segmentation," *IEEE Transactions on Multimedia*, 2020.
- [7] Y. Zeng, D. Cao, X. Wei, M. Liu, Z. Zhao, and Z. Qin, "Multi-modal relational graph for cross-modal video moment retrieval," in *Proceedings of the IEEE/CVF Conference on Computer Vision and Pattern Recognition*, 2021, pp. 2215–2224.
- [8] H. Shi, M. Hayat, and J. Cai, "Unpaired referring expression grounding via bidirectional cross-modal matching," *Neurocomputing*, vol. 518, pp. 39–49, 2023.
- [9] Y. Li, H. Qi, J. Dai, X. Ji, and Y. Wei, "Fully convolutional instance-aware semantic segmentation," in *2017 IEEE Conference on Computer Vision and Pattern Recognition, CVPR 2017, Honolulu, HI, USA, July 21-26, 2017*, 2017, pp. 4438–4446.
- [10] K. He, G. Gkioxari, P. Dollár, and R. Girshick, "Mask r-cnn," *IEEE Transactions on Pattern Analysis & Machine Intelligence*, vol. 42, no. 02, pp. 386–397, 2020.
- [11] Y. Du, F. Wei, Z. Zhang, M. Shi, Y. Gao, and G. Li, "Learning to prompt for open-vocabulary object detection with vision-language model," in *Proceedings of the IEEE/CVF Conference on Computer Vision and Pattern Recognition*, 2022, pp. 14 084–14 093.
- [12] M. Minderer, A. Gritsenko, A. Stone, M. Neumann, D. Weissenborn, A. Dosovitskiy, A. Mahendran, A. Arnab, M. Dehghani, Z. Shen *et al.*, "Simple open-vocabulary object detection with vision transformers," *European Conference on Computer Vision*, 2022.
- [13] A. Zareian, K. D. Rosa, D. H. Hu, and S.-F. Chang, "Open-vocabulary object detection using captions," in *Proceedings of the IEEE/CVF Conference on Computer Vision and Pattern Recognition*, 2021, pp. 14 393–14 402.
- [14] X. Gu, T.-Y. Lin, W. Kuo, and Y. Cui, "Open-vocabulary object detection via vision and language knowledge distillation," in *International Conference on Learning Representations*, 2022.
- [15] Z. Ma, G. Luo, J. Gao, L. Li, Y. Chen, S. Wang, C. Zhang, and W. Hu, "Open-vocabulary one-stage detection with hierarchical visual-language knowledge distillation," in *Proceedings of the IEEE/CVF Conference on Computer Vision and Pattern Recognition*, 2022, pp. 14 074–14 083.
- [16] J. Xu, S. Liu, A. Vahdat, B. Byeon, X. Wang, and S. De Mello, "Open-vocabulary panoptic segmentation with text-to-image diffusion models," in *Proceedings of the IEEE/CVF Conference on Computer Vision and Pattern Recognition*, 2023, pp. 2955–2966.
- [17] X. Zhou, R. Girdhar, A. Joulin, P. Krähenbühl, and I. Misra, "Detecting twenty-thousand classes using image-level supervision," *European Conference on Computer Vision*, 2022.
- [18] M. Gao, C. Xing, J. C. Niebles, J. Li, R. Xu, W. Liu, and C. Xiong, "Open vocabulary object detection with pseudo bounding-box labels," *European Conference on Computer Vision*, 2022.
- [19] D. Huynh, J. Kuen, Z. Lin, J. Gu, and E. Elhamifar, "Open-vocabulary instance segmentation via robust cross-modal pseudo-labeling," in *Proceedings of the IEEE/CVF Conference on Computer Vision and Pattern Recognition*, 2022, pp. 7020–7031.
- [20] W. Kuo, F. Bertsch, W. Li, A. Piergiovanni, M. Saffar, and A. Angelova, "Findit: Generalized localization with natural language queries," *European Conference on Computer Vision*, 2022.
- [21] L. H. Li, P. Zhang, H. Zhang, J. Yang, C. Li, Y. Zhong, L. Wang, L. Yuan, L. Zhang, J.-N. Hwang *et al.*, "Grounded language-image pre-training," in *Proceedings of the IEEE/CVF Conference on Computer Vision and Pattern Recognition*, 2022, pp. 10965–10975.
- [22] W. Zhang, J. Pang, K. Chen, and C. C. Loy, "K-net: Towards unified image segmentation," *Advances in Neural Information Processing Systems*, vol. 34, pp. 10 326–10 338, 2021.
- [23] H. Wang, Y. Zhu, H. Adam, A. Yuille, and L.-C. Chen, "Max-deeplab: End-to-end panoptic segmentation with mask transformers," in *Proceedings of the IEEE/CVF conference on computer vision and pattern recognition*, 2021, pp. 5463–5474.
- [24] B. Cheng, A. Schwing, and A. Kirillov, "Per-pixel classification is not all you need for semantic segmentation," *Advances in Neural Information Processing Systems*, vol. 34, pp. 17 864–17 875, 2021.
- [25] B. Cheng, I. Misra, A. G. Schwing, A. Kirillov, and R. Girdhar, "Masked-attention mask transformer for universal image segmentation," in *Proceedings of the IEEE/CVF Conference on Computer Vision and Pattern Recognition*, 2022, pp. 1290–1299.
- [26] J. Jain, J. Li, M. T. Chiu, A. Hassani, N. Orlov, and H. Shi, "Oneformer: One transformer to rule universal image segmentation," in *Proceedings of the IEEE/CVF Conference on Computer Vision and Pattern Recognition*, 2023, pp. 2989–2998.
- [27] T. Xu, W. Chen, W. Pichao, F. Wang, H. Li, and R. Jin, "Cdrans: Cross-domain transformer for unsupervised domain adaptation," in *International Conference on Learning Representations*, 2022.
- [28] R. Xie, F. Yu, J. Wang, Y. Wang, and L. Zhang, "Multi-level domain adaptive learning for cross-domain detection," in *Proceedings of the IEEE/CVF International Conference on Computer Vision Workshops*, 2019, pp. 0–0.
- [29] S. Ren, K. He, R. Girshick, and J. Sun, "Faster r-cnn: Towards real-time object detection with region proposal networks," *IEEE Transactions on Pattern Analysis & Machine Intelligence*, vol. 39, no. 06, pp. 1137–1149, 2017.
- [30] J. Redmon, S. K. Divvala, R. B. Girshick, and A. Farhadi, "You only look once: Unified, real-time object detection," in *2016 IEEE Conference on Computer Vision and Pattern Recognition, CVPR 2016, Las Vegas, NV, USA, June 27-30, 2016*, 2016, pp. 779–788.
- [31] W. Liu, D. Anguelov, D. Erhan, C. Szegedy, S. Reed, C.-Y. Fu, and A. C. Berg, "Ssd: Single shot multibox detector," in *European conference on computer vision*. Springer, 2016, pp. 21–37.
- [32] J. Long, E. Shelhamer, and T. Darrell, "Fully convolutional networks for semantic segmentation," in *Proceedings of the IEEE Conference on Computer Vision and Pattern Recognition*, 2015, pp. 3431–3440.
- [33] H. Shi, H. Li, Q. Wu, and Z. Song, "Scene parsing via integrated classification model and variance-based regularization," in *IEEE conference on computer vision and pattern recognition*, 2019.
- [34] L.-C. Chen, Y. Zhu, G. Papandreou, F. Schroff, and H. Adam, "Encoder-decoder with atrous separable convolution for semantic image segmentation," in *Proceedings of the European Conference on Computer Vision*, 2018.
- [35] H. Shi, M. Hayat, and J. Cai, "Transformer scale gate for semantic segmentation," in *Proceedings of the IEEE/CVF Conference on Computer Vision and Pattern Recognition*, 2023, pp. 3051–3060.
- [36] A. Kirillov, K. He, R. Girshick, C. Rother, and P. Dollár, "Panoptic segmentation," in *Proceedings of the IEEE/CVF Conference on Computer Vision and Pattern Recognition*, 2019, pp. 9404–9413.
- [37] A. Kirillov, R. Girshick, K. He, and P. Dollár, "Panoptic feature pyramid networks," in *Proceedings of the IEEE/CVF conference on computer vision and pattern recognition*, 2019, pp. 6399–6408.
- [38] Y. Xiong, R. Liao, H. Zhao, R. Hu, M. Bai, E. Yumer, and R. Urtaşun, "Upsnet: A unified panoptic segmentation network," in *Proceedings of the IEEE/CVF Conference on Computer Vision and Pattern Recognition*, 2019, pp. 8818–8826.
- [39] J. Dai, K. He, and J. Sun, "Instance-aware semantic segmentation via multi-task network cascades," in *2016 IEEE Conference on Computer Vision and Pattern Recognition, CVPR 2016, Las Vegas, NV, USA, June 27-30, 2016*, 2016, pp. 3150–3158.
- [40] T. Chen, S. Saxena, L. Li, D. J. Fleet, and G. Hinton, "Pix2seq: A language modeling framework for object detection," in *International Conference on Learning Representations*, 2022.
- [41] T. Chen, S. Saxena, L. Li, T.-Y. Lin, D. J. Fleet, and G. Hinton, "A unified sequence interface for vision tasks," in *Advances in Neural Information Processing Systems*, 2022.
- [42] A. Kolesnikov, A. S. Pinto, L. Beyer, X. Zhai, J. J. Harmsen, and N. Houlsby, "Uvim: A unified modeling approach for vision with learned guiding codes," in *Advances in Neural Information Processing Systems*, 2022.
- [43] X. Dong, Y. Zheng, J. Bao, T. Zhang, D. Chen, H. Yang, M. Zeng, W. Zhang, L. Yuan, D. Chen *et al.*, "Maskclip: Masked self-distillation advances contrastive language-image pretraining," *arXiv preprint arXiv:2208.12262*, 2022.
- [44] J. Xu, J. Hou, Y. Zhang, R. Feng, Y. Wang, Y. Qiao, and W. Xie, "Learning open-vocabulary semantic segmentation models from natural language supervision," *arXiv preprint arXiv:2301.09121*, 2023.

- [45] A. Radford, J. W. Kim, C. Hallacy, A. Ramesh, G. Goh, S. Agarwal, G. Sastry, A. Askell, P. Mishkin, J. Clark *et al.*, "Learning transferable visual models from natural language supervision," *arXiv preprint arXiv:2103.00020*, 2021.
- [46] Y. Zang, W. Li, K. Zhou, C. Huang, and C. C. Loy, "Open-vocabulary detr with conditional matching," *European Conference on Computer Vision*, 2022.
- [47] N. Carion, F. Massa, G. Synnaeve, N. Usunier, A. Kirillov, and S. Zagoruyko, "End-to-end object detection with transformers," in *European Conference on Computer Vision*. Springer, 2020, pp. 213–229.
- [48] W. Kuo, Y. Cui, X. Gu, A. Piergiovanni, and A. Angelova, "F-vlm: Open-vocabulary object detection upon frozen vision and language models," *International Conference on Learning Representations*, 2023.
- [49] C. Feng, Y. Zhong, Z. Jie, X. Chu, H. Ren, X. Wei, W. Xie, and L. Ma, "Promptdet: Towards open-vocabulary detection using uncurated images," in *European Conference on Computer Vision*, 2022, pp. 701–717.
- [50] Z. Ding, J. Wang, and Z. Tu, "Open-vocabulary panoptic segmentation with maskclip," *arxiv*, 2022.
- [51] Y. Zhong, J. Yang, P. Zhang, C. Li, N. Codella, L. H. Li, L. Zhou, X. Dai, L. Yuan, Y. Li *et al.*, "Regionclip: Region-based language-image pretraining," in *Proceedings of the IEEE/CVF Conference on Computer Vision and Pattern Recognition*, 2022, pp. 16793–16803.
- [52] S. Zhao, Z. Zhang, S. Schuster, L. Zhao, B. Vijay Kumar, A. Stathopoulos, M. Chandraker, and D. N. Metaxas, "Exploiting unlabeled data with vision and language models for object detection," in *European Conference on Computer Vision*, 2022, pp. 159–175.
- [53] C. Lin, P. Sun, Y. Jiang, P. Luo, L. Qu, G. Haffari, Z. Yuan, and J. Cai, "Learning object-language alignments for open-vocabulary object detection," *International Conference on Learning Representations*, 2023.
- [54] C. Zhou, C. C. Loy, and B. Dai, "Extract free dense labels from clip," *European Conference on Computer Vision*, 2022.
- [55] G. Ghiasi, X. Gu, Y. Cui, and T.-Y. Lin, "Scaling open-vocabulary image segmentation with image-level labels," *European Conference on Computer Vision*, 2022.
- [56] H. Rasheed, M. Maaz, M. U. Khattak, S. Khan, and F. S. Khan, "Bridging the gap between object and image-level representations for open-vocabulary detection," *Conference on Neural Information Processing Systems*, 2022.
- [57] Z. Cai, G. Kwon, A. Ravichandran, E. Bas, Z. Tu, R. Bhotika, and S. Soatto, "X-detr: A versatile architecture for instance-wise vision-language tasks," *European Conference on Computer Vision*, 2022.
- [58] H. Zhang, P. Zhang, X. Hu, Y.-C. Chen, L. H. Li, X. Dai, L. Wang, L. Yuan, J.-N. Hwang, and J. Gao, "Glipv2: Unifying localization and vision-language understanding," *Conference on Neural Information Processing Systems*, 2022.
- [59] X. Zou, Z.-Y. Dou, J. Yang, Z. Gan, L. Li, C. Li, X. Dai, H. Behl, J. Wang, L. Yuan *et al.*, "Generalized decoding for pixel, image, and language," *arXiv preprint arXiv:2212.11270*, 2022.
- [60] J. D. M.-W. C. Kenton and L. K. Toutanova, "Bert: Pre-training of deep bidirectional transformers for language understanding," in *Proceedings of NAACL-HLT*, 2019, pp. 4171–4186.
- [61] Y. Liu, M. Ott, N. Goyal, J. Du, M. Joshi, D. Chen, O. Levy, M. Lewis, L. Zettlemoyer, and V. Stoyanov, "Roberta: A robustly optimized bert pretraining approach," *arXiv preprint arXiv:1907.11692*, 2019.
- [62] K. Zhou, J. Yang, C. C. Loy, and Z. Liu, "Learning to prompt for vision-language models," *International Journal of Computer Vision*, vol. 130, no. 9, pp. 2337–2348, 2022.
- [63] K. He, X. Zhang, S. Ren, and J. Sun, "Deep residual learning for image recognition," in *Proceedings of the IEEE Conference on Computer Vision and Pattern Recognition*, 2016, pp. 770–778.
- [64] Z. Liu, Y. Lin, Y. Cao, H. Hu, Y. Wei, Z. Zhang, S. Lin, and B. Guo, "Swin transformer: Hierarchical vision transformer using shifted windows," *ICCV*, 2021.
- [65] X. Zhu, W. Su, L. Lu, B. Li, X. Wang, and J. Dai, "Deformable detr: Deformable transformers for end-to-end object detection," in *International Conference on Learning Representations*, 2021.
- [66] J. Xu, S. De Mello, S. Liu, W. Byeon, T. Breuel, J. Kautz, and X. Wang, "Groupvit: Semantic segmentation emerges from text supervision," in *Proceedings of the IEEE/CVF Conference on Computer Vision and Pattern Recognition*, 2022, pp. 18134–18144.
- [67] M. Xu, Z. Zhang, F. Wei, Y. Lin, Y. Cao, H. Hu, and X. Bai, "A simple baseline for open-vocabulary semantic segmentation with pre-trained vision-language model," in *European Conference on Computer Vision*, 2022, pp. 736–753.
- [68] F. Liang, B. Wu, X. Dai, K. Li, Y. Zhao, H. Zhang, P. Zhang, P. Vajda, and D. Marculescu, "Open-vocabulary semantic segmentation with mask-adapted clip," *arXiv preprint arXiv:2210.04150*, 2022.
- [69] R. A. Yeh, J. Xiong, W.-M. W. Hwu, M. N. Do, and A. G. Schwing, "Interpretable and globally optimal prediction for textual grounding using image concepts," *Advances in Neural Information Processing Systems*, 2017.
- [70] S. Kazemzadeh, V. Ordonez, M. Matten, and T. Berg, "Referitgame: Referring to objects in photographs of natural scenes," in *Conference on Empirical Methods in Natural Language Processing*, 2014, pp. 787–798.
- [71] R. Krishna, Y. Zhu, O. Groth, J. Johnson, K. Hata, J. Kravitz, S. Chen, Y. Kalantidis, L.-J. Li, D. A. Shamma *et al.*, "Visual genome: Connecting language and vision using crowdsourced dense image annotations," *IJCV*, 2016.
- [72] C. Wu, Z. Lin, S. Cohen, T. Bui, and S. Maji, "Phrasecut: Language-based image segmentation in the wild," in *Proceedings of the IEEE/CVF Conference on Computer Vision and Pattern Recognition*, 2020, pp. 10216–10225.
- [73] A. Gupta, P. Dollar, and R. Girshick, "Lvis: A dataset for large vocabulary instance segmentation," in *Proceedings of the IEEE/CVF conference on computer vision and pattern recognition*, 2019, pp. 5356–5364.
- [74] T.-Y. Lin, M. Maire, S. Belongie, J. Hays, P. Perona, D. Ramanan, P. Dollár, and C. L. Zitnick, "Microsoft coco: Common objects in context," in *Proceedings of the European Conference on Computer Vision*. Springer, 2014, pp. 740–755.
- [75] B. Zhou, H. Zhao, X. Puig, S. Fidler, A. Barriuso, and A. Torralba, "Scene parsing through ade20k dataset," in *Proceedings of the IEEE Conference on Computer Vision and Pattern Recognition*, 2017.
- [76] R. Mottaghi, X. Chen, X. Liu, N.-G. Cho, S.-W. Lee, S. Fidler, R. Urtasun, and A. Yuille, "The role of context for object detection and semantic segmentation in the wild," in *Proceedings of the IEEE Conference on Computer Vision and Pattern Recognition*, 2014, pp. 891–898.
- [77] A. Bansal, K. Sikka, G. Sharma, R. Chellappa, and A. Divakaran, "Zero-shot object detection," in *Proceedings of the European Conference on Computer Vision (ECCV)*, 2018, pp. 384–400.
- [78] A. Paszke, S. Gross, F. Massa, A. Lerer, J. Bradbury, G. Chanan, T. Killeen, Z. Lin, N. Gimelshein, L. Antiga *et al.*, "Pytorch: An imperative style, high-performance deep learning library," *Advances in neural information processing systems*, vol. 32, pp. 8026–8037, 2019.